

LEVEL

(3) fw

MPL TECHNICAL MEMORANDUM 307

14 MPL-TM-307
MPL-U-58/78

6 ADA CALIBRATION AT SEA

10 Victor C. Anderson
John C. Nickles

12 46

University of California, San Diego
Marine Physical Laboratory of the
Scripps Institution of Oceanography
San Diego, California 92152

DTIC
SELECTED
AUG 25 1981
H

AD A103670

9 Technical memo

Form Approved Budget Bureau No. 22R0293

Sponsored by
Advanced Research Projects Agency
ARPA Order Number 2426
Program Code Number 62702E

Administered by the Office of Naval Research

15 NO0014-75-C-0108, ARPA Order-
2426

Contract Effective Date: 1 July 1975

Contract Expiration Date: 15 November 1978

Amount of Advanced Detection Array Contract: \$2,971,003

11

F. N. Spiess/V. C. Anderson, (714) 452-2300/2304
Principal Investigator(s)

Scientific Officer: Director, Sensor Technology Program
Office of Naval Research
Department of the Navy

The views and conclusions contained in this document are those of the authors and should not be interpreted as necessarily representing the official policies, either expressed or implied, of the Advanced Research Projects Agency of the U.S. Government.

Document cleared for public release and sale; its distribution is unlimited.

DTIC FILE COPY

Approved: *Victor C. Anderson*
Victor C. Anderson

DISTRIBUTION STATEMENT A

Approved for public release;
Distribution Unlimited

MPL-U-58/78
MPL-U-58/78

217400

FILE COPY

81 8 25 074

met

Abstract

Calibration procedures for at-sea evaluation of the acoustic performance of the Advanced Detection Array (ADA) are discussed. The calibration data obtained during the June 1978 operation include measurements of location and wave-front errors across the array, large and small signal array gain, and effective spatial signal processing gain at several frequencies.

Accession For

NTIS GRA&I	<input checked="" type="checkbox"/>
DTIC TAB	<input type="checkbox"/>
Unannounced	<input type="checkbox"/>
Justification:	<i>also</i>
<i>FL-88 on file</i>	
By	
Distribution/	
Availability Codes	
Dist	Avail and/or Special
A	

1. INTRODUCTION

The measurement of array gain is of course essential to the interpretation of the results of detection experiments and background statistics measurements. The main emphasis of this report is on the measurements and analyses used to arrive both at the array gain, and at quantitative estimates of the sources of discrepancies between expected and measured performance. Illustrative data from the June, 1978 seatrip are presented.

The detailed investigation of sensitivity, frequency response and directional pattern of individual hydrophones is not a part of normal at-sea operations and is not included here. Such hydrophone calibrations were reported in Ref. 1. On the other hand, operations do include a check on the status of each hydrophone and the selection of correctly operating elements for use in beamforming. This procedure is described in Section II. The measurement of element position errors and wavefront distortion, which affect the proper phasing of the element outputs, is discussed in Section III.

The array gain measurement is done in two parts: the peak response to large signals is a direct measure of the ability of the array and beamformer to operate as a spatial filter, and is considered in Section IV, while the on-axis

NPL-U-58/78

gain of the array for small signals (in the linear operating range of the DIMUS processor) is described in Section V. Section VI summarizes and relates the procedures and results described in the preceding sections. A list of related reports is included at the end.

II. ELEMENT CALIBRATION AND SELECTION

The first step in the operation of ADA, once it is submerged, is to measure the signal response and the noise output of each array element, and to identify the elements which are not working properly. The beamformer inputs for the faulty elements are then inhibited before any array gain measurements or processing experiments are started. The hydrophone survey and selection process may be repeated several times during the operation, and a final verification run is made before the array is surfaced. The measurements and the analysis are automated so that the selection can be completed in a reasonable time. Typically, the whole procedure takes about three hours.

1. Experimental measurement.

The system provides for the monitoring and digital recording of the outputs of any two selected hydrophones, at either the input or the output of the digital filter. For the element selection process, one of these cal/mon (calibrate/monitor) channels is held fixed on a manually selected reference hydrophone; the second is connected to each of the 720 hydrophones in turn. Digital filter outputs are used.

For the signal response, the array is oriented toward

NPL -U-58/78

URB and a sound source suspended from URB at approximately the same depth as ADA. The computer generates 100 msec tone bursts at either 1250 or 2500 Hz; these are amplified and drive the suspended source. The digital filter is programmed for either the 1150 to 1350 Hz or the 2400 to 2600 Hz band, as appropriate.

The selection process depends only on the response of each element relative to the selected reference phone, and not on absolute sensitivity, so the drive level and signal conditioner gain are adjusted to give a good signal-to-noise ratio, while avoiding overloads in either the driver or the array electronics.

The pulse repetition rate is varied, depending on water depth, array depth, and range from the source to ADA, to avoid interference from reflected arrivals. Between pulses, the computer changes selection of the test hydrophone. Typically a 1.0 to 1.5 second interval is used, so that the scan of the 720 elements may require twelve to eighteen minutes. After a delay to allow for the pulse travel time, cal/mon outputs of both the test and reference channels are recorded. The record is made long enough to be sure to include the entire pulse arrival, allowing for some variation in the array position while the elements are scanned.

NPL-U-59/78

Element noise outputs are measured using the same program, but with the driver turned off. The 800-3200 Hz digital filter is selected. The array is directed away from ORB, to eliminate machinery noise. The record length for each hydrophone is 0.5 seconds, so that the scan takes six minutes.

2. Data reduction.

The recorded data are processed by programs which read the tapes and produce disk files containing relative signal response or noise power for each hydrophone. The signal response program uses a cross correlation filter to extract the signal at the test frequency, in 25 msec intervals. The correlation sums are stored on an intermediate disk file, which may be used to produce a calibration report, if desired. For the selection procedure, this file is read by a program which tests the reference channel power for successive 25 msec intervals until the leading edge of the pulse is found. Then the data for a 75 msec interval are coherently combined, and the power is calculated and converted to decibels for both the test and the reference channels. The difference is stored in the relative signal response file for input to the selection program.

For noise, the time samples for each channel are squared

NPL-U-58/78

and averaged over a 300 msec interval, and stored in an intermediate file. This data is then converted to noise power relative to the reference phone. The noise may optionally be normalized by the signal response to yield the equivalent input noise. Again, the result in dB is stored in a disk file which will serve as input to the selection program. For this 300 msec integration time, the expected error in the noise power estimate for the 800-3200 Hz band is 0.23 dB.

4. Selection procedure.

The processed data files from these runs are read by a program which prints, or displays for the operator, a histogram of the relative response or noise measurements. From these, upper and lower acceptance limits for good hydrophones may be selected. The selection program generates a file which has three status indicators for each hydrophone: one for signal response at each frequency, and one for noise. Initially, the indicators are all cleared. As each of the processed data files is read, the appropriate indicator is set for every element whose response falls within the specified limits. The final selection of hydrophones to be used by the beamformer requires all three status indicators to be set.

NPL-U-58/78

In order not to reject good hydrophones because of a single bad reading, two signal response runs at each frequency and two noise power runs are made. The selection status indicator will be set if either of the two readings meets the selection criterion. The assumption is that the probability of the same good element being rejected by two independent measurements is small, and that the chance that a bad hydrophone will be accepted on at least one run on each type of measurement is also small.

4. Results and analysis.

A page of the relative response summary for the 2 June 1978 hydrophone selection is reproduced in Fig. II.1. This report is not used in the selection process, but is examined to ensure that the results of the measurements and the first stages of processing are reasonable. Table II.1 shows the response distributions from which the operator chooses acceptance limits. The vertical bars indicates the limits which were used in this case.

Two-dimensional histograms of the same runs are shown in Figs. II.2. These show a reasonable consistency between runs, i. e., most of the measurement pairs are clustered along the diagonal, where the two measurements are nearly equal. We can use these histograms to justify, in an

02-JUN-78 18 10 09 1750 HZ		02-JUN-78 18 22 19 2500 HZ		02-JUN-78 18 39 44 2500 HZ		02-JUN-78 19 01 47 NOTISE		02-JUN-78 19 12 03 NOTISE	
M 0	RESP 0.7	M 0	RESP 0.5	M 0	RESP 0.3	M 0	RESP 2.1	M 0	RESP 1.9
M 1	RESP 0.7	M 1	RESP 1.0	M 1	RESP 0.7	M 1	RESP 1.2	M 1	RESP 1.7
M 2	RESP -0.3	M 2	RESP 0.7	M 2	RESP -0.1	M 2	RESP 1.2	M 2	RESP 0.4
M 3	RESP -2.4	M 3	RESP -2.3	M 3	RESP 0.0	M 3	RESP 6.1	M 3	RESP 1.2
M 4	RESP 1.4	M 4	RESP 4.2	M 4	RESP 1.0	M 4	RESP 2.5	M 4	RESP 2.8
M 5	RESP 0.4	M 5	RESP -0.3	M 5	RESP -0.3	M 5	RESP 2.5	M 5	RESP 2.8
M 6	RESP -0.1	M 6	RESP 0.5	M 6	RESP 0.6	M 6	RESP 2.5	M 6	RESP -0.1
M 7	RESP -2.2	M 7	RESP -1.9	M 7	RESP -1.8	M 7	RESP 2.7	M 7	RESP 5.1
M 8	RESP 1.7	M 8	RESP 1.0	M 8	RESP 0.3	M 8	RESP 0.4	M 8	RESP 1.1
M 9	RESP 1.4	M 9	RESP 3.8	M 9	RESP 0.7	M 9	RESP 1.6	M 9	RESP 1.1
M 10	RESP -5.0	M 10	RESP -2.4	M 10	RESP -2.9	M 10	RESP 1.2	M 10	RESP 1.1
M 11	RESP 0.7	M 11	RESP 1.5	M 11	RESP 1.1	M 11	RESP -2.2	M 11	RESP 5.9
M 12	RESP 0.1	M 12	RESP 4.1	M 12	RESP 0.6	M 12	RESP 2.7	M 12	RESP 11.5
M 13	RESP -0.1	M 13	RESP 0.2	M 13	RESP -0.3	M 13	RESP 1.8	M 13	RESP 2.7
M 14	RESP 0.7	M 14	RESP -0.4	M 14	RESP 0.1	M 14	RESP 1.6	M 14	RESP 0.5
M 15	RESP 0.7	M 15	RESP -0.4	M 15	RESP -0.2	M 15	RESP 1.6	M 15	RESP 2.4
M 16	RESP -2.1	M 16	RESP -2.7	M 16	RESP -0.2	M 16	RESP 2.1	M 16	RESP 7.4
M 17	RESP -1.4	M 17	RESP -2.9	M 17	RESP -0.4	M 17	RESP 2.9	M 17	RESP 1.9
M 18	RESP 2.9	M 18	RESP -0.2	M 18	RESP -0.2	M 18	RESP 2.9	M 18	RESP 3.2
M 19	RESP 2.9	M 19	RESP -1.3	M 19	RESP -1.5	M 19	RESP 9.7	M 19	RESP 1.5
M 20	RESP 1.1	M 20	RESP -5.3	M 20	RESP -4.9	M 20	RESP 3.4	M 20	RESP 10.2
M 21	RESP -1.9	M 21	RESP 0.8	M 21	RESP -1.9	M 21	RESP 24.9	M 21	RESP 4.1
M 22	RESP 0.9	M 22	RESP 0.8	M 22	RESP -0.1	M 22	RESP 1.7	M 22	RESP 2.9
M 23	RESP 0.1	M 23	RESP 0.2	M 23	RESP 0.6	M 23	RESP 1.9	M 23	RESP 2.0
M 24	RESP -1.8	M 24	RESP -1.7	M 24	RESP -0.6	M 24	RESP -3.0	M 24	RESP 2.0
M 25	RESP 1.0	M 25	RESP 4.7	M 25	RESP -0.4	M 25	RESP 1.4	M 25	RESP -1.7
M 26	RESP 0.9	M 26	RESP 2.2	M 26	RESP 1.4	M 26	RESP 1.4	M 26	RESP 1.7
M 27	RESP 0.7	M 27	RESP 1.4	M 27	RESP 1.7	M 27	RESP 9.2	M 27	RESP 11.2
M 28	RESP 0.5	M 28	RESP 5.5	M 28	RESP -0.2	M 28	RESP 0.8	M 28	RESP 2.4
M 29	RESP -0.4	M 29	RESP 4.0	M 29	RESP 0.1	M 29	RESP 2.8	M 29	RESP 0.9
M 30	RESP -0.1	M 30	RESP 0.4	M 30	RESP 0.2	M 30	RESP 0.9	M 30	RESP 0.7
M 31	RESP -2.2	M 31	RESP -7.9	M 31	RESP -4.2	M 31	RESP 4.2	M 31	RESP 4.5
M 32	RESP 0.6	M 32	RESP -0.4	M 32	RESP 0.2	M 32	RESP -10.7	M 32	RESP -10.9
M 33	RESP 0.5	M 33	RESP 1.5	M 33	RESP 0.2	M 33	RESP 0.9	M 33	RESP 0.9
M 34	RESP 1.4	M 34	RESP 0.3	M 34	RESP -1.1	M 34	RESP 12.1	M 34	RESP 12.2
M 35	RESP 2.8	M 35	RESP 0.2	M 35	RESP 0.2	M 35	RESP 2.5	M 35	RESP 2.3
M 36	RESP -0.1	M 36	RESP 0.2	M 36	RESP -1.4	M 36	RESP 5.2	M 36	RESP 4.2
M 37	RESP 1.4	M 37	RESP 0.7	M 37	RESP -0.9	M 37	RESP 6.0	M 37	RESP 6.0
M 38	RESP 1.9	M 38	RESP 4.7	M 38	RESP 1.2	M 38	RESP 8.7	M 38	RESP 2.3
M 39	RESP 3.9	M 39	RESP 1.2	M 39	RESP 1.1	M 39	RESP 10.6	M 39	RESP 6.0
M 40	RESP 4.4	M 40	RESP -5.1	M 40	RESP -4.6	M 40	RESP 10.6	M 40	RESP 11.0
M 41	RESP -0.4	M 41	RESP 0.2	M 41	RESP -1.5	M 41	RESP 0.5	M 41	RESP 0.4
M 42	RESP 1.9	M 42	RESP 4.4	M 42	RESP 0.7	M 42	RESP 7.7	M 42	RESP 10.4
M 43	RESP 0.5	M 43	RESP 0.5	M 43	RESP 1.2	M 43	RESP 6.7	M 43	RESP 6.9
M 44	RESP -0.4	M 44	RESP -3.8	M 44	RESP -4.6	M 44	RESP 6.7	M 44	RESP 6.9
M 45	RESP 0.9	M 45	RESP 0.6	M 45	RESP -0.8	M 45	RESP 14.2	M 45	RESP 4.2
M 46	RESP 1.5	M 46	RESP -5.8	M 46	RESP -0.8	M 46	RESP 2.3	M 46	RESP 2.9
M 47	RESP 0.3	M 47	RESP 0.4	M 47	RESP -0.1	M 47	RESP 1.8	M 47	RESP 1.4
M 48	RESP 1.0	M 48	RESP 0.7	M 48	RESP 0.9	M 48	RESP 1.6	M 48	RESP 1.4
M 49	RESP 1.1	M 49	RESP -0.1	M 49	RESP -0.5	M 49	RESP 1.4	M 49	RESP 1.4
M 50	RESP 1.7	M 50	RESP 1.9	M 50	RESP 1.3	M 50	RESP 2.1	M 50	RESP 2.1
M 51	RESP 1.7	M 51	RESP 1.7	M 51	RESP -0.5	M 51	RESP 2.0	M 51	RESP 2.1
M 52	RESP 0.7	M 52	RESP 2.3	M 52	RESP 0.7	M 52	RESP 4.0	M 52	RESP 1.0
M 53	RESP 0.1	M 53	RESP 0.7	M 53	RESP 1.1	M 53	RESP 0.6	M 53	RESP 4.2
M 54	RESP -0.4	M 54	RESP 0.0	M 54	RESP 0.0	M 54	RESP 0.6	M 54	RESP 0.4
M 55	RESP 1.9	M 55	RESP 3.1	M 55	RESP -0.2	M 55	RESP 0.7	M 55	RESP 0.3
M 56	RESP 2.6	M 56	RESP 11.2	M 56	RESP 1.5	M 56	RESP 1.6	M 56	RESP 1.4
M 57	RESP -0.6	M 57	RESP -3.7	M 57	RESP 19.9	M 57	RESP 21.0	M 57	RESP 20.9
M 58	RESP -1.4	M 58	RESP -1.8	M 58	RESP -2.4	M 58	RESP 7.9	M 58	RESP 8.5
M 59	RESP -0.1	M 59	RESP -0.9	M 59	RESP 1.9	M 59	RESP 3.7	M 59	RESP 4.1
M 60	RESP -0.5	M 60	RESP 0.7	M 60	RESP 0.3	M 60	RESP 12.8	M 60	RESP 6.1
M 61	RESP 0.7	M 61	RESP 0.7	M 61	RESP 0.3	M 61	RESP 0.3	M 61	RESP 0.5

Figure II.1 Relative Response Summary

Relative Response	1250 Hz		2500 Hz		NOISE	
	RUN 1	RUN 2	RUN 1	RUN 2	RUN 1	RUN 2
≤ -10	43	43	59	47	13	9
- 9	2	0	2	1	2	1
- 8	0	1	2	6	0	2
- 7	1	1	1	7	2	0
- 6	2	3	11	10	1	1
- 5	1	2	16	9	0	2
- 4	2	4	12	11	2	2
- 3	8	10	21	13	3	0
- 2	14	12	43	18	3	5
- 1	39	49	117	100	9	11
0	214	203	239	263	199	169
1	241	245	120	168	193	172
2	117	108	43	52	77	88
3	17	21	7	9	31	47
4	6	6	7	0	33	39
5	4	4	5	1	25	21
6	2	2	3	0	23	28
7	2	2	2	1	17	17
8	2	1	0	0	12	21
9	1	2	0	1	13	7
≥ 10	2	1	10	3	62	78

Table II.1 Response distribution

NPL-U-58/78

informal way, our earlier claim that the selection is not likely to reject a good hydrophone. For example, at 1250 Hz, 672 hydrophones are within the acceptance limits for one or both runs, while ten are in limits for Run 1 only, and nine for Run 2 only. This means that the probability of rejecting a good phone on a single run is roughly $10/672$ or 0.015, and that of rejecting a good phone on two independent runs is only about 0.00022.

Figure II.3 is a printout showing which hydrophones were inhibited by the selection procedure for this data. The asterisks indicate the rejected elements.

FOR HYDROPHOBIC KILLER DATA FILE
 32-JUN-78 00 00 00

16	17	18	19*	20	21*	22	23	24*	25	26	27*	28	29	30	31	15	14	13	12	11*	10*	9	8	7	6	5	4	3	2	1	0
32*	33	34*	35	36	37	38	39	40*	41	42	43	44	45*	46	47																
48	49	50*	51	52	53	54	55	56*	57	58	59	60	61	62	63																
64	65	66	67	68	69	70*	71	72	73*	74	75	76	77	78	79																
80	81	82	83*	84	85	86	87	88*	89	90	91	92	93	94	95																
96	97	98*	99	100	101	102	103	104	105	106*	107*	108	109	110	111*																
112	113	114	115*	116	117	118*	119	120	121	122	123	124	125	126*	127																
128	129	130	131	132*	133	134*	135*	136*	137	138*	139	140	141	142	143																
144	145	146*	147	148	149	150	151	152	153	154	155	156	157	158	159																
160	161	162	163	164	165	166	167	168*	169*	170	171*	172	173	174	175*																
176	177*	178	179	180*	181	182	183	184	185	186*	187*	188	189	190	191																
192	193	194*	195	196	197	198	199*	200	201	202	203*	204*	205	206	207																
208	209	210	211	212	213	214	215	216	217	218	219	220	221	222	223*																
224	225	226	227	228	229	230	231	232	233	234	235	236	237	238	239*																
240	241	242	243	244	245	246	247	248*	249	250	251*	252	253	254	255																
256*	257	258	259	260*	261	262	263	264	265	266	267	268	269	270*	271*																
272	273	274	275*	276	277	278	279	280	281	282	283	284	285*	286*	287																
288	289	290	291	292	293	294	295	296*	297*	298	299	300	301	302	303																
304	305	306	307*	308	309	310	311	312	313	314	315	316	317	318	319*																
320	321	322	323*	324	325	326	327	328	329	330	331*	332	333	334	335																
336	337	338*	339	340	341	342*	343	344	345	346	347	348	349	350	351*																
352	353	354	355	356	357	358	359	360	361	362	363	364	365	366	367																
368	369	370	371	372	373	374	375	376	377*	378	379	380	381	382*	383																
384	385	386	387*	388	389	390	391*	392	393	394	395	396	397	398	399																
400*	401	402	403	404	405	406	407	408	409*	410	411	412	413	414*	415																
416*	417	418	419	420	421	422	423	424*	425	426	427	428	429	430	431																
432	433	434	435	436	437*	438	439	440	441	442	443*	444	445	446	447*																
448	449	450	451	452	453	454	455	456	457	458	459	460	461	462	463*																
464	465	466	467	468	469	470*	471	472	473	474	475	476	477	478	479																
480	481	482	483	484	485*	486	487	488	489	490	491	492	493	494	495																
496	497	498	499	500*	501	502	503	504	505	506	507	508	509	510	511																
512	513	514	515	516	517	518	519	520	521	522	523	524	525	526	527																
528	529	530	531	532	533	534	535	536	537	538	539*	540	541	542*	543																
544*	545*	546	547	548	549*	550	551	552	553	554*	555	556*	557	558*	559																
560	561*	562	563	564	565*	566	567	568	569	570	571	572	573	574	575																
576	577	578	579	580	581	582	583*	584	585*	586	587	588*	589	590	591																
592*	593	594	595	596	597	598	599	600	601	602	603	604	605	606	607																
608	609	610	611	612*	613	614*	615	616	617	618	619	620	621	622	623																
624	625	626	627*	628	629	630	631	632	633	634*	635	636	637	638	639																
640	641	642	643	644	645	646	647*	648	649	650	651	652	653	654	655*																
656	657	658	659*	660	661	662	663	664*	665	666	667	668*	669*	670	671																
672	673	674	675*	676	677	678	679	680	681	682	683	684*	685	686	687*																
688	689*	690	691	692	693	694	695	696	697	698	699	700	701	702	703*																
704*	705	706	707	708	709	710	711*	712	713	714*	715	716*	717	718	719																

103 MAD HYDROPHOBES

Figure II.3 Killer data file listing

NPL-U-58/78

III. ELEMENT POSITION ERRORS AND DOME DISTORTION

Errors in arrival times at the various array elements, relative to the times which would be expected for a plane wave, arise for two reasons: the true element positions are not exactly known, and the wavefront is distorted by the water mass enclosed by the dome. The position errors are primarily due to the compliant mounts, which do not stand exactly perpendicular to the deck; additional errors may arise from varying mount lengths and possible bending or buckling of the deck when the array is at depth. The water in the dome is less saline than seawater, and does not come to thermal equilibrium until the array has been submerged for a long time.

1. Experimental measurement.

The arrival times are measured using an experimental setup similar to that for the element signal response measurements. The primary difference is in the element selection sequence. Again, one cal/mon channel is held fixed on a selected reference phone while the other is connected to each element in turn. The analysis program will use the difference between the arrival times at the test and reference elements as a measure of element position error and/or wavefront distortion.

MPL-U-58/78

The errors of primary interest in connection with the investigation of array gain are those perpendicular to the plane of the array. For these, the measurement is made with the array oriented toward the source. However, since the array is not entirely stationary during the measurements, it is necessary to have a concurrent measurement of the angle of incidence of the wavefront with respect to the plane of the array. For this purpose, two pairs of additional reference elements are chosen: one with elements at each end of the array near the horizontal centerline, the other with elements at the top and bottom near the vertical centerline. The selection sequence is interrupted at regular intervals, and records for the horizontal and vertical pairs are included.

The signal frequency used is 2700 Hz. This has been selected empirically to give a reproducible waveform with a well-defined leading edge. The one octave digital filter band from 1600 to 3200 Hz is used, since a narrow band filter would alter the shape of the leading edge.

2. Arrival time determination.

The data tapes are read by a program which measures the arrival time on each cal/mon channel and stores these in a disk file for further analysis. The operator monitors this initial analysis with a display as shown in Fig. III.1.

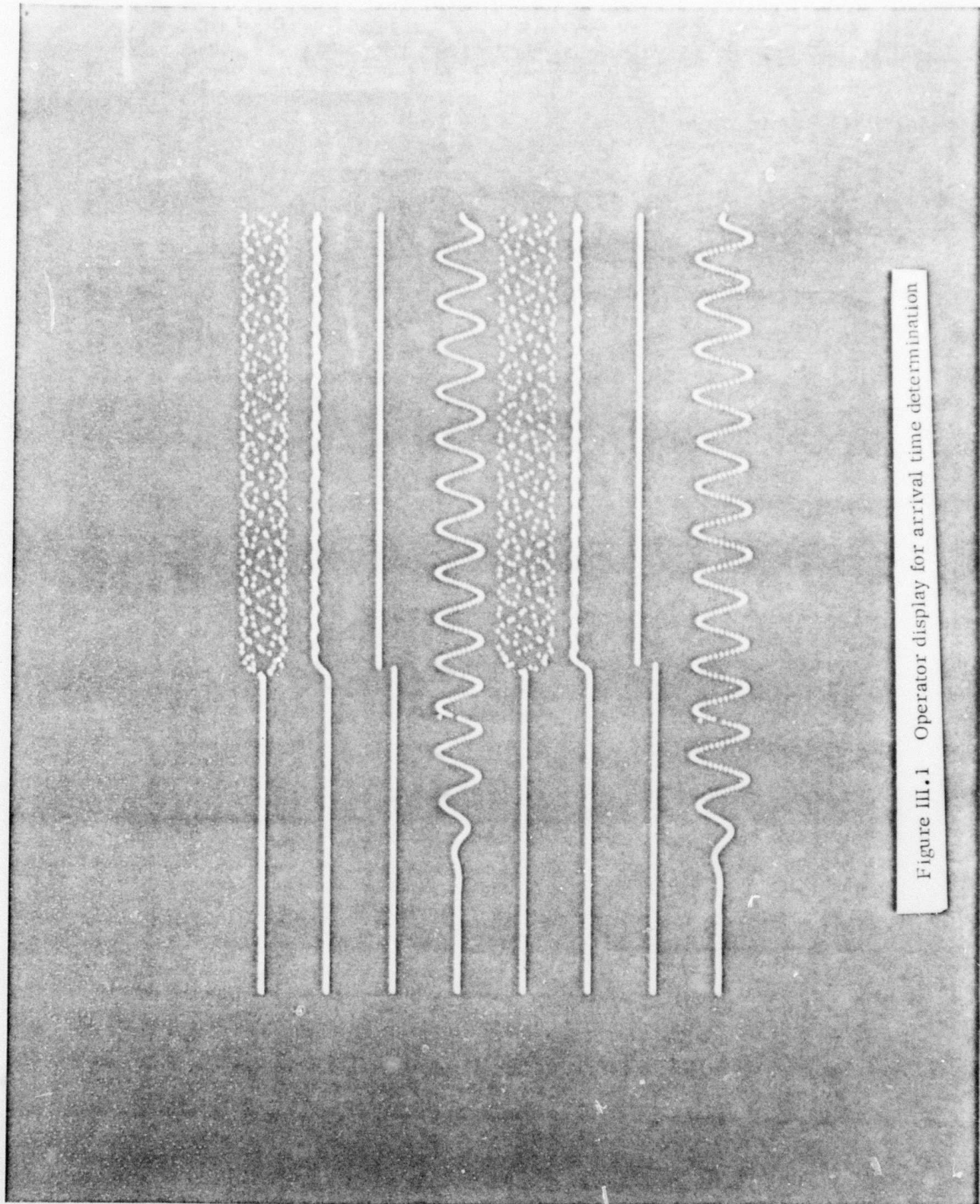


Figure III.1 Operator display for arrival time determination

NPL U-58/78

Eight traces are shown, four for each of the two cal/mon channels. The upper trace of each set of four is a 51.2 msec (512 sample) "window" of the data from the tape. The recorded data includes from one to four records of 1024 samples, and the operator must manually position the data window within this larger set of data. This means that the program does not need to deal with multiple arrivals, and helps the operator feel needed. Of course, the pulse repetition rate must be set when the data is recorded to keep surface or bottom bounce arrivals from interfering with the direct arrival.

The second trace is the envelope of the signal, obtained by exponentially averaging the absolute value of the recorded data. The averaging time was experimentally adjusted to give a reasonable compromise between leading edge definition and noise rejection. The envelope data is scanned for the peak level, then again for the position of the first sample which exceeds half the peak. This gives an approximate measure of the position of the leading edge. The third trace is a step function whose height is the peak envelope amplitude and whose transition occurs at the leading edge of the pulse, as determined by the program.

To get a better measure of the position of the leading

NPL-U-58/78

edge of the pulse, the program uses an interpolation algorithm to expand the time scale in the region near the edge by a factor of eight. Sixty-four points (16 before and 48 after the edge) are expanded to 512 points and displayed in the fourth trace. The effective sample rate for the interpolated data is 80 kHz, which gives a position resolution of 1.8 cm.

The program must now search for a point in the waveform which may be reliably identified. For this particular waveform, the first negative peak seems to be a good choice. To make the measurement reasonably independent of element sensitivity, the peak is identified by comparing the data to a threshold which is one third of the peak envelope level. This threshold was empirically chosen to give as reliable an identification as possible.

The leading edge of the pulse is not a particularly good point for determining the arrival time. More reproducible results are obtained by counting several cycles into the pulse to get beyond the transient response, which is not closely matched from element to element. The program finds the positive-going axis crossing following the third negative peak. This point is identified on the display by a vertical offset, and its position is the final measure of arrival

NPI-U-58/78

time. The axis crossing is used because the time determination is most precise where the slope is a maximum.

3. Time difference error determination.

The next step in the processing is to compare the measured arrival time at each element (relative to the reference hydrophone), to the expected time computed from the nominal position of the element. The expected arrival time is of course dependent on the direction of the source relative to the array, so two passes are made through the travel time data file. First, the program looks only at the data for the horizontal and vertical reference pairs. From these, it calculates and stores the components of a unit vector normal to the wavefront. On the second pass, the relative arrival time for each element is compared to an expected value obtained by interpolating between the stored vector components.

4. Results and analysis.

Figure III.2 is a listing of the position error estimates for a typical run. Each pair of columns lists hydrophone numbers, from 0 to 719, together with the estimated position error, in centimeters. The asterisks indicate hydrophones for which the program could not make a position estimate or which had been previously masked out of

MPL-U-58/78

the array in the hydrophone selection process. Most of the errors are clustered near zero. Some, however, are in the vicinity of 28 cm (a half wavelength at 2700 Hz) or 56 cm (one wavelength). The one wavelength errors result from a failure of the program to correctly identify the first cycle of the received pulse; these points were not numerous and were ignored in the subsequent statistical analysis of the data. On the other hand, the half wavelength errors turn out to identify hydrophones whose outputs are phase reversed; this was verified by examining the recorded waveform for several such cases. There were ten phase reversed hydrophones, and they were inhibited during the remainder of the operation.

In order to investigate the reproducibility of these measurements, position error estimates from three independent runs have been compared. The absolute value of the difference between pairs of estimates for the same hydrophone has been calculated, and a histogram of these differences is shown in Fig. III.3. Ninety percent of them are 3 cm or less. The agreement between the data for the three runs has been used as a selection criterion for the statistical analyses which follow. A position error is rejected as invalid if it is greater than 20 cm (probably indicating a

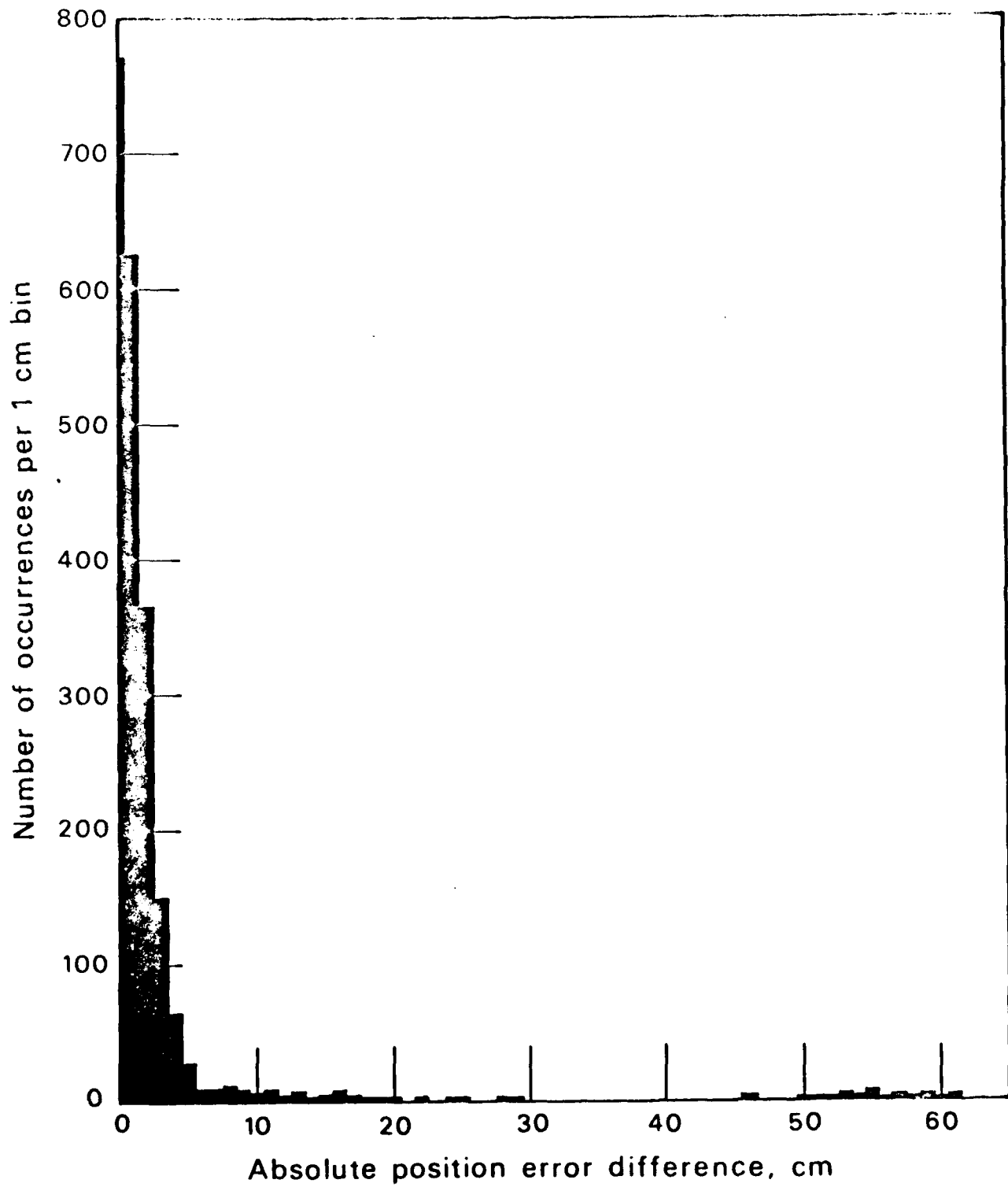


Figure III.3 Histogram of run-to-run differences between position error estimates

HPL-U-58/78

phase reversal or a one wavelength measurement error) or if it does not agree with at least one of the other two runs within 4 cm.

Using this criterion, the mean position error has been found to be 2.12 cm. Since the positions are relative, this merely represents the distance of the reference hydrophone from the mean array plane and is not important. The two statistics which are significant are the RMS deviation and the mean absolute deviation of the hydrophones from the mean array plane. These are 1.87 and 1.49 cm, respectively. The mean absolute error affects the peak beam response, as discussed in Section IV, while the RMS error is significant for the prediction of loss of array gain for small signals, which will be considered in Section V.

We can consider the apparent position errors to arise from two sources: a random physical position error due to imperfect mounts and structure, and a systematic part resulting from the wavefront distortion at the dome. To isolate the dome effect, in table III.1 we have considered the array to be divided into eleven horizontal slices, each 60 cm high. The mean position error for each slice is listed. Also shown is the expected error of the mean, based on the number of elements in the slice and the 1.87 cm

y	$N(y)$	$\bar{z}(y)$	$\sigma_{\bar{z}}(y)$
-330 to -270 cm	8	- .75 cm	.71 cm
-270 to -210	31	- .19	.34
-210 to -150	50	.29	.27
-150 to -90	73	.24	.22
-90 to -30	80	.23	.21
-30 to +30	101	.20	.19
+30 to +90	77	.55	.21
+90 to +150	72	- .26	.22
+150 to +210	53	- .64	.26
+210 to +270	29	-1.49	.35
+270 to +330	11	- .47	.59

Table III.1 Vertical dependence of position error

NPL-U-58/78

standard deviation for the whole array. The standard deviation of the set of 11 means is only 0.56 cm, so the wavefront distortion does not contribute a major portion of the total position error.

NPL-U-58/78

IV. PEAK BEAM RESPONSE AT HIGH SIGNAL TO NOISE RATIO

The ability of the array and beamformer to correctly recombine a coherent waveform is measured by training the array toward the source suspended from ORB, transmitting pulses at a high enough level so that the clipped beamformer input statistics are dominated by the signal during the pulse arrival, and continuously recording the short term average (STA) beam scan. A 100 msec pulse is used so that it always encompasses the full 50 msec integration time of at least one STA sample.

The data tape is read by a program which selects and prints the largest beam output, both as an absolute level and as a fraction of the maximum possible output. It also prints the beam azimuth and elevation in both true and relative coordinate systems. This printout is scanned to find the pulse arrivals, and these readings are recorded for hand analysis.

The source level is set to produce a signal-to-noise ratio at the hydrophone outputs of approximately +10 dB. Measurements have been carried out at 1.3, 1.75 and 2.5 kHz, corresponding to frequencies transmitted by the towed source during the June operation.

Because each beam response is a maximum only in a single

NPL-U-58/78

direction and is somewhat reduced at angles between adjacent beam centers, there is a problem in trying to make precise measurements of peak beam response if the arrival happens to be at such an intermediate angle. It was expected that small random motions of the array would negate this effect if the measurement were repeated several times, and the largest value used. However, during the analysis of the first trial run of this measurement, it was found that this was not the case, particularly with regard to the beam elevation angle. The problem was solved by creating a special beam set, covering a smaller total solid angle, with the beams tightly packed near the source direction.

The peak beam response was measured again, and the result was still much lower than expected, suggesting that the phasing was in error. To check this possibility, the following test was devised. The beamformer was reprogrammed by loading it with the coordinates of an hypothetical array with elements on a regular grid, and the test signal generator was enabled, so that the signal conditioner inputs were driven with a sinusoidal signal. This should result in a response pattern which has large grating lobes produced by constructive interference at certain angles. In fact, these lobes turned out to be smaller than predicted.

NPL -U-58/78

By using different sets of steered beams, it was possible to isolate the problem to one of the three beamformer sections. Fig. IV.1 shows the peak grating lobe level for beamformer A, which was working correctly, and beamformer C, which was not. The frequencies used were chosen to be incommensurate with the 10 kHz sample rate, since otherwise the phase errors are not random and exact phasing occurs. The theoretical response for a uniformly distributed phase error and an absolute value detector is shown for comparison.

The error was found, after the operation, to be caused by a bad integrated circuit multiplier which was not detected during the system checkout. The faulty chip has been replaced, and the checkout program has been modified.

The peak beam response was measured using beamformer A only. The results are plotted in Fig. IV.2 as a function of relative bearing angle. Note that the peak beam response shows little or no dependence on angle. The theoretical levels shown are again calculated for uniformly distributed phase errors and an absolute value detector. The measured values are roughly 1 dB below the theoretical levels. The on-axis measurement at 1300 Hz falls very close to the theoretical curve. However, this sample occurred on the

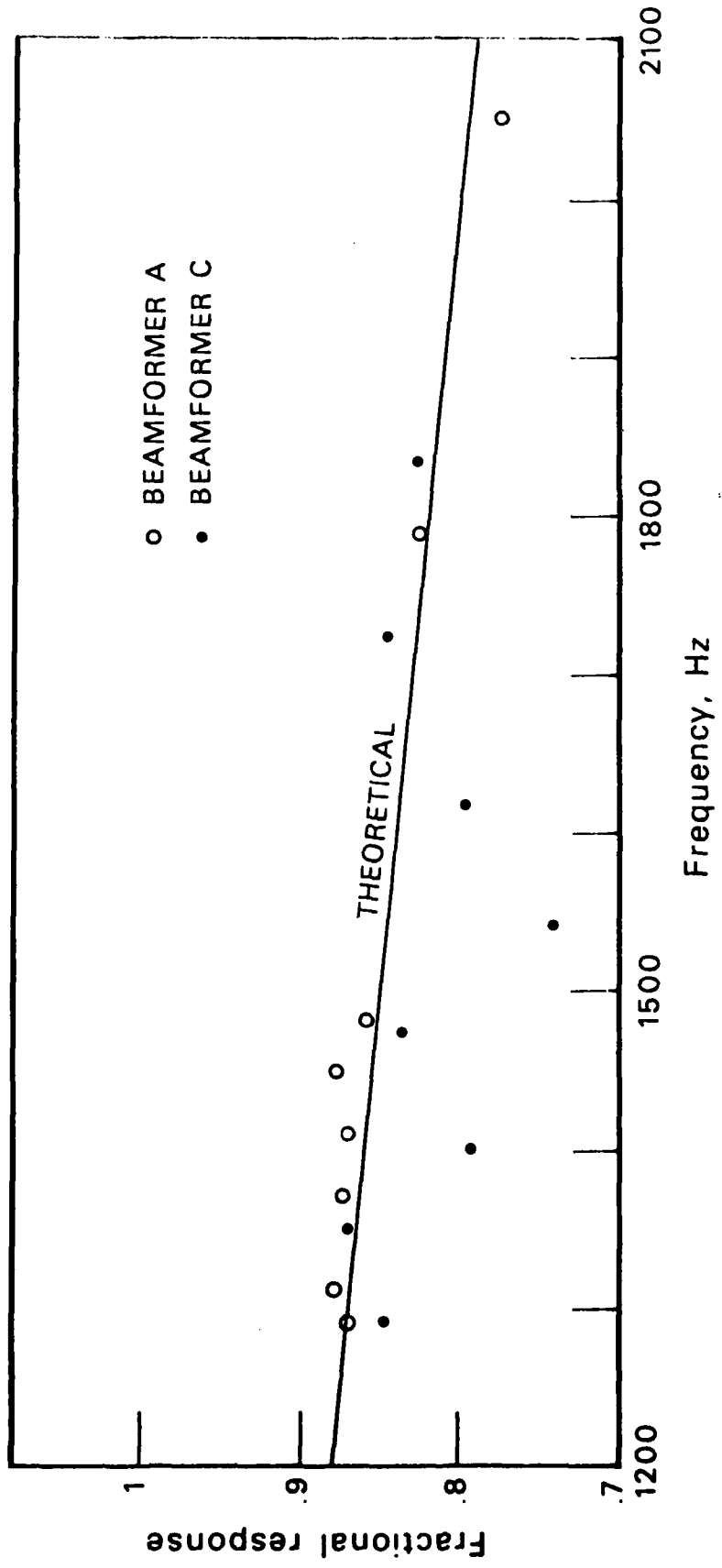


Figure IV.1 Peak grating lobe levels for beamformers A and C

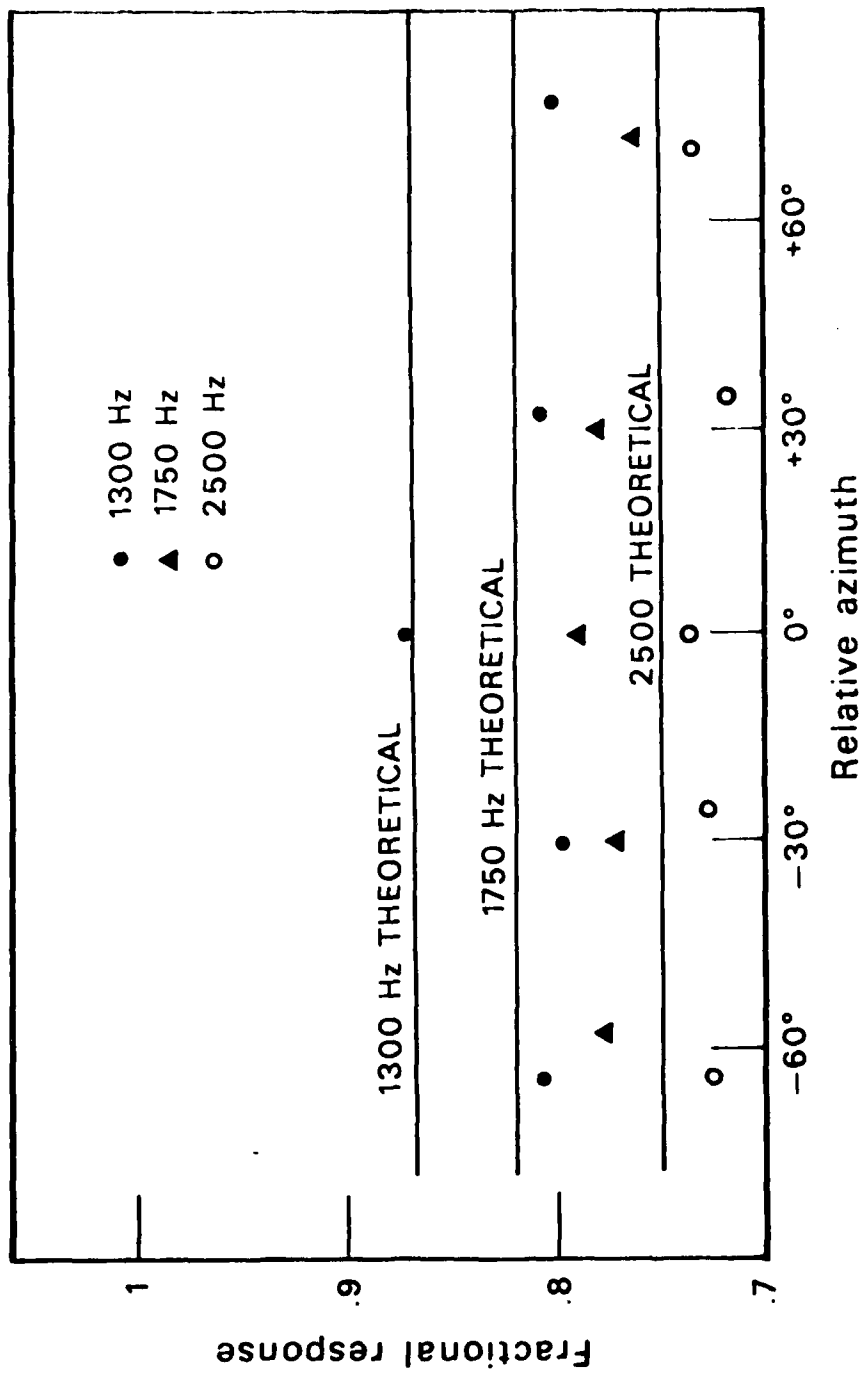


Figure IV.2 Peak beam response vs azimuth

MPL-U-58/78

broadside beam, where the time delays generated by the beamformer are zero and the phase error is not randomly distributed over the full range of 2π . For this case the theoretical peak response could approach unity.

The measurement of hydrophone position errors and wavefront distortion at the dome was discussed in Section III. The mean absolute error in the direction normal to the plane of the array was found to be 1.49 cm. At 2500 Hz, this is 0.0248 wavelength, and should reduce the peak response by only 2.5 percent. The reduction is even smaller at the lower frequencies.

MPL -U-58/78

V. ON-AXIS ARRAY GAIN FOR SMALL SIGNALS

The measurement discussed in this section was made using a sound source suspended from a ship at ranges from 5 to 12 kiloyards. The transmitted signal was a superposition of sinusoids at 1.0, 1.3, 1.75, and 2.5 kHz. The undetected outputs of a single hydrophone and a beam trained on the source were recorded. The power spectra of the recorded data were then computed and plotted, as illustrated in Fig. V.1. This data can be interpreted in two different ways, which we shall discuss in turn.

1. System sensitivity.

Here we want to consider the sensitivity in a way analogous to the calibration of a hydrophone. A fundamental property of the DIMUS system is that the inputs to the beamformer are perfectly normalized, i. e., the clipped signals have constant power. Clearly, then, the sensitivity is not just a property of the system, but depends on the nature of the acoustic environment. For a signal which is small compared to the noise (at the hydrophone outputs) the system is nearly linear, so the beam output can be used as a measure of absolute signal level.

First, however, the beam outputs must be denormalized by multiplying them by the signal level at the clipper inputs.

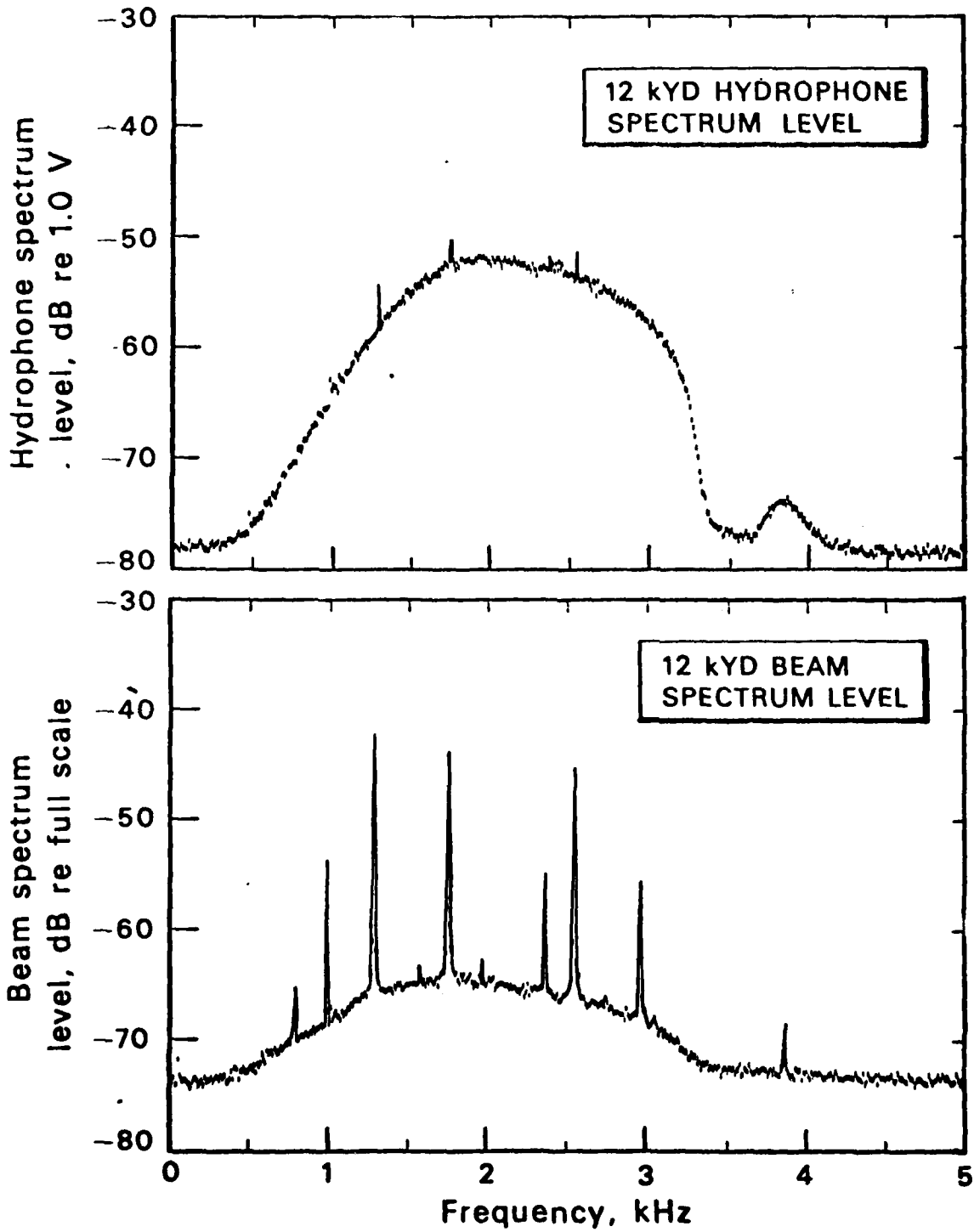


Figure V.1 Element and beam spectra

MPL-U-58/78

and corrected by a frequency dependent gain factor to correct for the beamformer losses, including clipping. In the ideal case this factor would just be the $\pi/2$ clipping loss. The hydrophone response, in the direction of arrival of the signal, must then be applied to arrive at the signal sound pressure level. These corrections are not made by the system hardware, but must be done after the fact if, for example, we want to use the array to measure sound pressure levels in connection with a propagation loss experiment.

The plotted spectra have been used to calculate the frequency-dependent beamformer gain factor. The calculation is summarized in Table V.I. The first two columns of the table identify the data record and the frequency. LB and NB are the line level and noise level for the beam, and CLB is the beam line level corrected for the noise. Since the beam signal-to-noise level is high, the correction is small. LE, NE and CLE are the analogous levels for the element; in this case the corrections are more significant. The RMS element output is available in the header of the spectrum plot. This is used to denormalize the beamformer line level, and the result is listed in the column labeled DLB. Finally, the beamformer gain is obtained by subtracting the input (CLE) from the denormalized output (DLB).

Record I.D.	Freq (Mhz)	Beam Line Level			Element Line Level			Denormalization			Beamformer Gain
		LB	NB	CLB	LE	NE	CLLE	RMS	DLB	DLB	
11:51:44	1.3	-33.5	-50	-38.2	-49.0	-57.0	-49.7	-15.5	-53.7	-4.0	
	1.7	-31.5	-48	-31.5	-41.0	-51.0	-41.5	"	-47.0	-5.5	
	2.5	-30.5	-49	-30.5	-39.0	-53.0	-39.3	"	-46.0	-6.7	
05:16:17	1.3	-39.0	-58	-39.0	-51.0	-56.5	-52.5	-15.7	-54.7	-2.2	
	1.7	-36.0	-58	-36.0	-45.5	-50.5	-47.0	"	-51.7	-4.7	
	2.5	-37.5	-59	-37.5	-46.0	-52.0	-47.2	"	-53.2	-6.0	
04:57:20	1.0	-45.0	-68	-45.0	-57.0	-64.0	-58.0	-16.4	-61.4	-3.4	
	1.3	-42.5	-65	-42.5	-53.5	-57.5	-56.0	"	-58.9	-2.9	
	1.7	-30.0	-62	-30.0	-42.0	-51.5	-42.5	"	-46.4	-3.9	
04:43:20	2.5	-31.5	-60	-31.5	-43.0	-53.0	-43.5	"	-47.9	-4.4	
	1.3	-42.5	-65	-42.5	-54.2	-58.5	-56.2	-17.3	-59.8	-3.6	
	1.7	-43.8	-65	-43.8	-50.0	-52.0	-54.3	"	-61.1	-6.8	
	2.5	-45.0	-66	-45.0	-51.0	-53.5	-54.7	"	-62.3	-7.6	

Table V.1 Beamformer gain factor calculation

MPL-U-58/78

If the gain factors are averaged at each frequency, the result is -3.4 dB at 1.0 kHz, -3.2 dB at 1.3 kHz, -5.7 dB at 1.75 kHz, and -6.2 dB at 2.5 kHz. While only one reading was obtained at 1.0 kHz, the readings at the other frequencies for the same data record are above the averages, and we may at least hope that the beam was well trained on the target and that the 1.0 kHz reading is valid.

For comparison, the theoretical DIMUS clipping loss is -2 dB. An additional correction should be made because the reference level for the plotted beam spectra is full scale peak amplitude, and should really be RMS amplitude. If we assume this correction is approximately 3 dB (which would be correct for a sinusoidal waveform) the expected gain would be -5 dB, which lies within the range of measured values. The lower gain values obtained at higher frequencies can probably be ascribed to not having the audio beam steered exactly on the source, which would affect the higher frequencies more strongly because of the narrower beam. For the 04:57:20 record, the frequency dependence is less pronounced; the beam may have been better trained on the target.

The average gain factors listed above were used in the analysis of the propagation loss estimates used in Ref. 5.

2. Spatial processing gain.

Alternatively, the plotted spectra may be used to calculate the processing gain, i. e., the gain in signal-to-noise ratio, provided by the beamformer. The signal-to-noise ratios at the outputs of the hydrophone and the beam, for each of the source lines, are read from the plots and compared. Naturally, the spectral lines include both signal and noise, and this effect must be corrected to get true signal-to-noise ratio. For example, if the ratio of signal-plus-noise to noise is 1 dB, the signal itself is about 10 dB below the noise. In this case, very small variations in signal-plus-noise will produce large changes in the result. Since what we are trying to measure is the gain for signals which are small at the hydrophone outputs, the careful selection of data is essential.

The spectrum analysis program corrects the data for the analysis bin width, so that we actually have spectrum level rather than line level. However, this applies to both the element and the beam data, and does not affect their difference.

The calculated processing gain for several data points at each of the four source frequencies is plotted in Fig. V.2. The 1.6 to 3.2 kHz digital filter was in use when this data was taken, and as a result the values obtained at 1.0

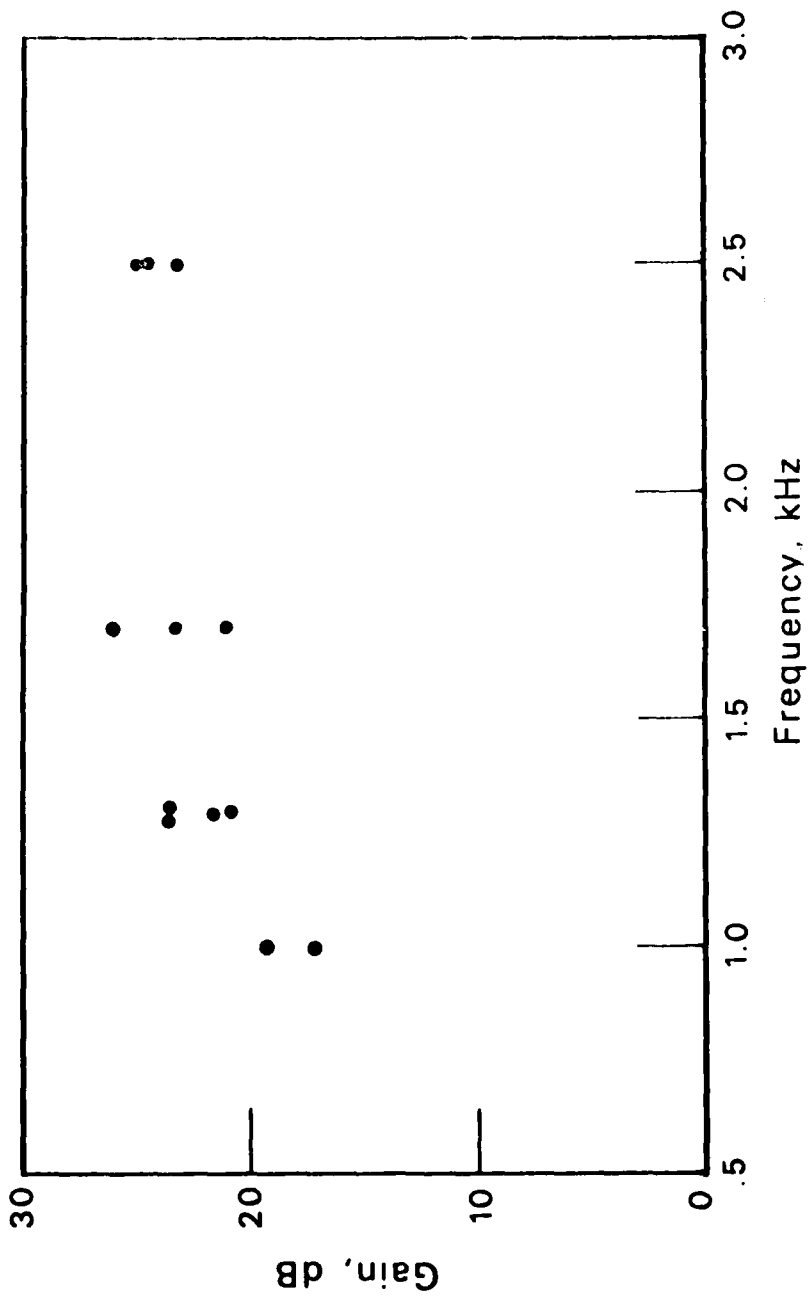


Figure V.2 ADA spatial processing gain

NPL-U-58/78

and 1.3 kHz represent out-of-band processing gains which are lower than would apply if the system were operated with the low band or wideband filter. The reason is that, although the filter reduces the low frequency components for both the hydrophone and the beam data, the beamformer clipper noise will have a greater relative contribution than it would otherwise, and will reduce the measured array gain.

It should be noted that this array gain is measured with respect to the hydrophone outputs and so does not include the directivity index of the hydrophones themselves. The effective noise directivity index of the receiving elements was determined by comparing the outputs from a hydrophone operating in the directional mode and in the omni mode with a 200 Hz wide 1 kHz center frequency filter band. These measurements, made online with an RMS voltmeter, indicated that the effective directivity index of the element was 4.5 dB.

VI. SUMMARY AND CONCLUSIONS

Element position measurements confirmed that the deviation of the array elements from the wavefront of an acoustic wave normal to the deck had an overall RMS value of 1.87 cm, which is a phase error of .13 radians at 2.5 kHz. The effect of these deviations would be expected to reduce the array gain by 0.14 dB.

Peak beam response at high signal-to-noise ratio yielded responses which fell below the theoretically expected results by about 1 dB. This difference indicates that there may be some residual hardware deficiencies because the precision of generating a sum with a high signal-to-noise ratio should be quite high. However, the excellent agreement with expected grating lobe response obtained with the simulator input would indicate that any deficiency was not in the beamformer, but in the hydrophone system.

Small signal beam sensitivity measurements provide the system calibration factors required to infer acoustic line levels from beam output spectra. These factors were the ones used to compute propagation loss in the detection experiment of Ref. 5.

The effective spatial processing gain of the array as determined by a comparison of simultaneously measured signal

NPL-U-58/78

line levels and broad band noise spectrum levels on an element and on a beam output yields in-band processing gains of about 24 dB. This is 1 dB lower than the theoretical gain of 25 dB for a DIMUS processor, with the 513 elements used in the measurement. This 1 dB difference is consistent with the results of the high signal-to-noise peak beam response measurements.

The overall spatial processing gain of the array is the sum of the hydrophone directional gain and the array gain, $24 + 4.5 = 29.5$ dB.

References

1. J. A. Presley, Report of ADA Preliminary Calibration Results (Sea trip May 31 through June 6, 1977), MPL Tech Memo 296, 15 September 1977.
An initial report on at sea hydrophone calibration measurements
2. V. C. Anderson, ADA Experimental Program - Guidelines for Experimental Measurements, MPL Tech Memo 283 A&B, 1 April 1977(A), 11 May 1977 (B).
A summary of the ADA acoustic system (Part A) and a discussion of experimental measurement plans (Part B)
3. V. C. Anderson, Data Collection and Analysis Plan for the June 1978 ADA Operation, MPL Tech Memo 299, 12 June 1978.
Data collection and analysis plan for the June deep water operations
4. V. C. Anderson, A Controlled Source Detection Experiment with ADA June 8, 1977 (U), MPL-S-59/78.
Analysis of a portion of the June detector experiment with a towed sound source
5. V. C. Anderson, Nonstationary and Nonuniform Oceanic Background in a High Gain Acoustic Array, MPL-U-21.1/78.
Analysis of deep water directional noise spectra from a 4 hour observation period, June 12, 1978

